Relations between albedos and emissivities from MODIS and ASTER data over North African Desert

L. Zhou,[1] R. E. Dickinson,[1] K. Ogawa,[2] Y. Tian,[1] M. Jin,[3] T. Schmugge,[2] and E. Tsvetsinskaya[4]

Received 28 June 2003; revised 19 August 2003; accepted 25 August 2003; published 17 October 2003.

[1] This paper analyzes relations among MODIS surface albedos, ASTER broadband (3–14 μm) emissivities, and a soil taxonomy map over the arid areas of Algeria, Libya, and Tunisia in North Africa at 30 second (about 1 km) and 2 minute (about 4 km) spatial resolutions. The MODIS albedo data are from 7 spectral bands and 3 broadbands during dust-free seasons and the emissivity data are derived from a linear combination of the waveband emissivities of the ASTER five thermal infrared channels. Both albedo and emissivity data in the study region show similar considerable spatial variability, larger than assumed by most climate models, and such variability is related to the surface types (sands, rock, and soil orders). Emissivity over bare soils exhibits statistically significant correlations with albedos at both broadbands and most of spectral bands and decreases linearly with albedos. Albedo and emissivity are more strongly correlated with each other than either is to the surface types, apparently because of their higher resolution either spatially or in surface mineralogy. This paper provides guidance for the possible inclusion of such correlation to specify albedo and emissivity in climate models. *INDEX TERMS:* 1620 Global Change: Climate dynamics (3309); 1640 Global Change: Remote sensing; 3307 Meteorology and Atmospheric Dynamics: Boundary layer processes; 3322 Meteorology and Atmospheric Dynamics: Land/atmosphere interactions; 3337 Meteorology and Atmospheric Dynamics: Numerical modeling and data assimilation; *KEYWORDS:* Emissivity, Albedo, MODIS, ASTER. **Citation:** Zhou, L., R. E. Dickinson, K. Ogawa, Y. Tian, M. Jin, T. Schmugge, and E. Tsvetsinskaya, Relations between albedos and emissivities from MODIS and ASTER data over North African Desert, *Geophys. Res. Lett.*, *30*(20), 2026, doi:10.1029/2003GL018069, 2003.

1. Introduction

[2] Emissivity is defined as the ratio of thermal radiation emitted by a surface to that of a blackbody and albedo is defined as the fraction of incident solar energy reflected by the land surface in all directions. They determine the surface radiation budget, and thus the sensible, latent, and ground heat fluxes, and consequently important climate variables such as temperature and precipitation [*Dickinson et al.*, 1993; *Bonan et al.*, 2002].

[3] As two key parameters in climate models, emissivity and albedo have been only crudely represented due to limited observations. For example, a constant emissivity of 0.96 is used for bare soils in the recently developed Common Land Model [*Zeng et al.*, 2002] and NCAR Community Land Model [*Bonan et al.*, 2002]. Bare soil albedos in these two models are specified by soil wetness and 8 soil colors globally from dark to light. Such simple representations lose much spatial and spectral information.

[4] Unlike what has been included in climate models up to now, considerable spatial variability in surface albedo and emissivity over deserts and semi-deserts is observed from satellite derived data [*Tsvetsinskaya et al.*, 2002; *Ogawa et al.*, 2003a, 2003b; *Zhou et al.*, 2003]. Soils, sands, and rock are generally classified as a single land cover type in climate model deserts such as the Sahara. However, solar shortwave diffuse albedos vary by a factor of about 2.5 from the darkest volcanic terrains to the brightest sand sheets [*Tsvetsinskaya et al.*, 2002] and window emissivities (8–12μm) range from 0.81 to 0.99 in the Sahara [*Ogawa et al.*, 2003a]. Therefore, climate models may need to consider the spatial variations of surface emissivity and albedo.

[5] *Tsvetsinskaya et al.* [2002] have shown how satellite measured albedos can be applied to characterize the albedos of northern Africa. They find that, in the absence of vegetation, spatial variability in its surface albedos is largely related to the soil units as obtained from the 1994 FAO-UNESCO world soil classification map [*FAO*, 1994] and geographical characteristics. Since both emissivity and albedo depend on the same surface, can a similar relationship as that of *Tsvetsinskaya et al.* [2002] be obtained for emissivity? If so, then the surface types (i.e., sands, rock, and soil types) could be prescribed as boundary conditions and used in GCM to represent emissivity as well as albedo. Are they highly correlated? If so, how much of this correlation is related to the underlying surface type?

[6] Climate models could use a consistent scheme of albedo and emissivity based on the surface types. To consider this possibility, this paper analyzes the relations among ASTER broadband emissivity, MODIS albedos, and a soil taxonomy map over the arid areas in North Africa at 30 second (about 1 km) and 2 minute (about 4 km) spatial resolutions.

2. Data and Methods

[7] A study region of 520 × 1400 km^2 over Algeria, Libya, and Tunisia in North Africa is selected for its wide

[1]School of Earth and Atmospheric Sciences, Georgia Institute of Technology, Atlanta, Georgia, USA.
[2]USDA/ARS Hydrology and Remote Sensing Lab., Beltsville, Maryland, USA.
[3]Department of Meteorology, University of Maryland, College Park, Maryland, USA.
[4]Department of Geography, Boston University, Boston, Massachusetts, USA.

0094-8276/03/2003GL018069$05.00

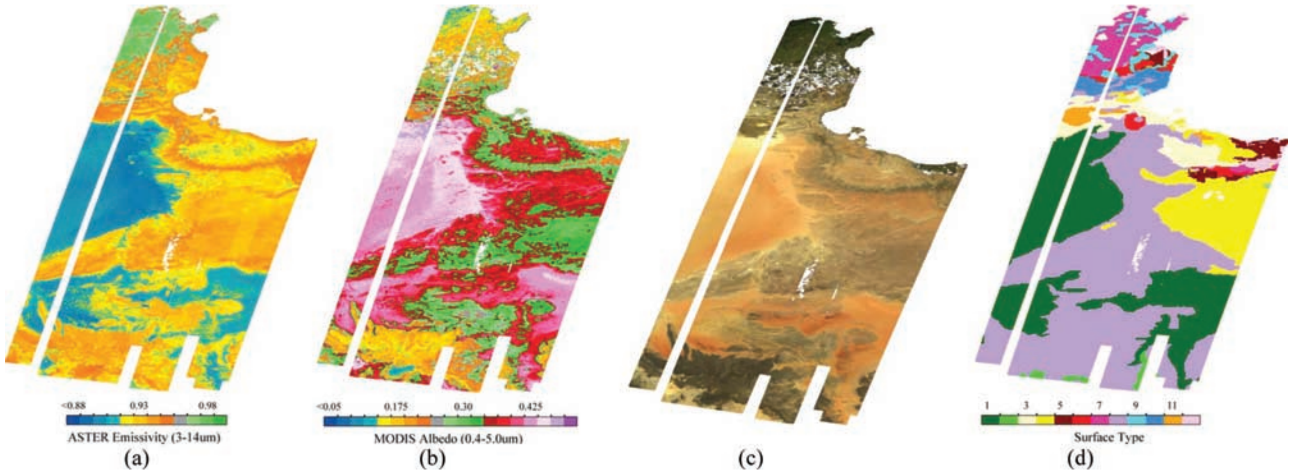

Figure 1. Spatial patterns of (a) ASTER emissivity, (b) MODIS albedo (0.4–5.0 μm), (c) true-color RGB image from MODIS black-sky albedos in red, green, and blue bands, and (d) the soil taxonomy over the study region at 30 second resolution. Each surface type in (d) is defined in Table 1.

variety of land cover. We use the MODIS albedo product (MOD43B3, validated version V003) in 2001 for 7 spectral bands and 3 broadbands [*Schaaf et al.*, 2002] averaged over dust-free periods from November through January. The MODIS albedos represent the best quality retrieval possible from the multidate multiangular cloud-free atmospherically corrected surface reflectances at 1-km resolution over each 16-day period. They consist of local noon black-sky (direct) and white-sky (diffuse) albedos. Since the white-sky albedos vary spatially as do the black-sky albedos, only results of the latter are shown here.

[8] The broadband emissivity (3–14 μm) data was derived from a linear combination of the ASTER five channel emissivities at 30 second resolution, with a residual error of less than 0.005 [*Ogawa et al.*, 2003a]. A total of 258 ASTER scenes at 90 m resolution were acquired from 2000 to 2002 to cover the study area. ASTER has more spectral bands in the 8–12 μm range (window region) than MODIS and thus may give a more reliable spectral to broadband emissivity conversion. The latter has only one channel in 8–9.5 μm where the largest range of emissivity is observed [*Ogawa et al.*, 2003b]. As an independent data set, the former helps support our analyses of MODIS albedo.

[9] We use a soil taxonomy map at 2 minute resolution [*Soil Survey Staff*, 1999], based on a reclassification of the 1994 FAO-UNESCO soil map of the world combined with a soil climate map. It consists of 12 major soil orders and 64 suborders globally. The FAO-UNESCO soil map has been established broadly to map soils at a continental scale and the total variation within each class is large. On a regional scale, the soil taxonomy map may be more suitable. There are 10 soil suborders over the study region. For simplicity, these soil suborders, together with shifting sands and rock, are referred as the surface types.

[10] All the data are reprojected to 30 second and 2 minute resolutions. The former is used to illustrate data spatial variability and the latter is used to better assess the association between the surface types and satellite observations. Since vegetation is heterogeneous and varies seasonally in deserts and semideserts, we adopt the purity concept of *Tian et al.* [2002] to retain only non-vegetated pixels with a purity of 100%, i.e., each of these 2 minute pixels contains only non-vegetated subpixels based on MODIS 1 km land cover map [*Friedl et al.*, 2002].

3. Results

[11] Figure 1 shows spatial distributions of ASTER emissivity, MODIS broadband albedo (0.4–5.0 μm), a RGB true-color image, and the soil taxonomy map over the study region at 30 second resolution. The RGB image, composited from MODIS red (0.62–0.67 μm), green (0.545–0.565 μm), and blue (0.459–0.479 μm) black-sky albedos, visualizes the soil surface. It has a close visual resemblance to the soil taxonomy map, suggesting the latter may have been derived in part from some previous remote sensing imagery but of lower resolution than MODIS. Evidently, the albedo and emissivity are tightly linked in spatial pattern and magnitude and clearly reveal details in surface soil texture and geological characteristics. Their spatial variations are generally consistent with those of the surface types. Pixels with the lowest emissivities (blue in Figure 1a) are those with the highest albedos (pink and purple in Figure 1b), belonging to the same surface type: shifting sands (orange in Figure 1c and green in Figure 1d). The vegetated regions in the northwest (Figure 1c) have the maximum emissivities and minimum albedos. Such connections of emissivity to albedo can be also found for other surface types.

[12] Figure 2 illustrates the histograms of albedo and emissivity (Figures 1a and 1b) for three surface types, 1 (brightest, shifting sand), 12 (darkest, xerolls), and 8 (dominant, orthents), with total pixels of 187820, 6806, and 316591, respectively. Albedo ranges from 0.09 to 0.49 and emissivity from 0.88 to 0.99. Shifting sands are the most reflective (0.399 ± 0.054) and least radiative (0.908 ± 0.010) of surfaces while xerolls have the least reflection (0.233 ± 0.054) and the most radiation (0.947 ± 0.090). Orthents, the most abundant soil type in the study region,

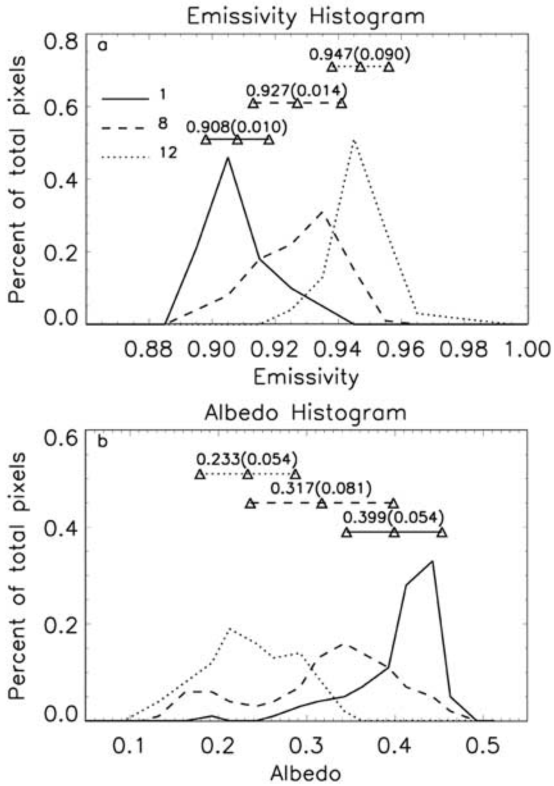

Figure 2. Histograms for (a) ASTER emissivity and (b) MODIS albedo (0.4–5.0 μm) at 30 second resolution for the surface types 1 (shifting sand), 8 (orthents), and 12 (xerolls). The symbol "Δ" represents means and standard deviations for each surface type.

are intermediate, with a wider spread around the means (0.927 ± 0.014 for emissivity and 0.317 ± 0.081 for albedo).

3.1. Surface Type Control of Albedo and Emissivity Connection

[13] Table 1 lists means and standard deviations (STDs) of broadband albedo (0.4–5.0 μm) and emissivity over non-vegetated 2 minute pixels by surface type. The means and STDs are about 0.26–0.40 and less than 0.08 for albedos, and about 0.91–0.95 and less than 0.01 for emissivity, respectively. The brightest surface (shifting sands) has the lowest emissivity while the darkest soil (xerolls) has the highest emissivity. Figure 3a plots the means of emissivity versus those of broadband albedo (0.4–5.0 μm) for each surface type, and Figure 3b plots values of emissivity versus broadband albedo for all pixels (35507) and shows a linear fit (R^2 = 0.58, $p < 0.01$). Similar correlations (not shown) are also seen between emissivity and other MODIS broadband and spectral band albedos.

Table 1. Mean and Standard Deviation of MODIS Albedos (0.4–5.0 μm) and ASTER Emissivity by Surface Type

Surface Types[a]				
No:	Name	Albedo	Emissivity	Pixels
1	Shifting sand	.401(.049)	.908(.010)	11210
3	Gypsids	.356(.056)	.927(.014)	1999
4	Calcids	.355(.026)	.929(.007)	3754
5	Ustalfs	.348(.030)	.928(.007)	294
6	Ustepts	.342(.045)	.931(.011)	309
7	Xerepts	.341(.026)	.930(.006)	85
8	Orthents	.326(.076)	.926(.013)	16939
9	Fluvents	.318(.041)	.933(.009)	33
10	Cambids	.311(.037)	.937(.010)	74
11	Argids	.304(.076)	.938(.012)	469
2	Rock	.299(.071)	.927(.009)	301
12	Xerolls	.263(.030)	.946(.005)	40

[a]Sorted by the magnitude of albedo means.

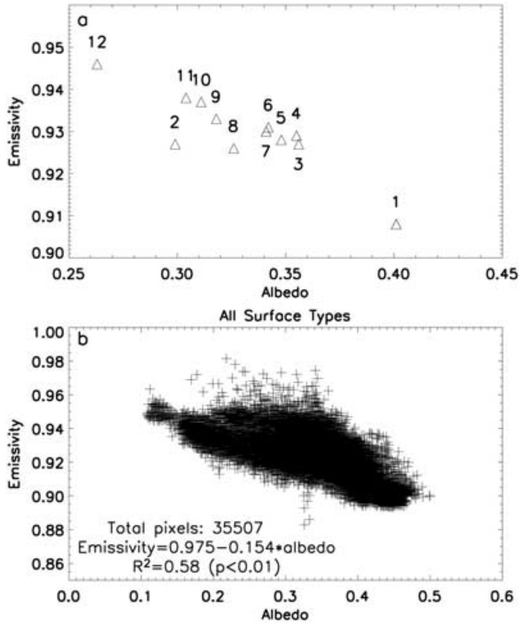

Figure 3. Relations between ASTER emissivity and MODIS albedo (0.4–5.0 μm) over non-vegetated 2 minute pixels: (a) means by surface type (b) scatter plot for all pixels.

[14] The Analysis of Variance (ANOVA) can be used to quantify the dependence of albedo and emissivity on the underlying surface type. The total variance of emissivity or albedo can be partitioned into variances of between and within surface types. We can test whether the surface types control spatial variability of albedo and emissivity (i.e., the means of the surface types are different). Table 2 shows that the surface types can explain both broadband albedo and emissivity variations at the 1% significance level but that much of their variance is within the surface types.

3.2. Linkage Between Albedo and Emissivity

[15] The association between albedo and emissivity can be quantified by their spatial correlation. The correlation coefficient between Figures 1a and 1b is −0.78. Table 3 lists correlation coefficients between ASTER broadband emissivity and albedos of MODIS 7 spectral bands and 3 broadbands over non-vegetated 2 minute pixels by surface type.

Table 2. ANOVA Table for MODIS Albedos and ASTER Emissivity

	Variance (Sum of squares)		F
Albedo(0.4–5.0 μm)	Between surface type	40.5	935($p < .01$)
	Within surface type	139.6	
Emissivity	Between surface type	2.9	2044($p < .01$)
	Within surface type	4.5	

Table 3. Correlations Between MODIS Albedos and ASTER Emissivity by Surface Type

MODIS bands (μm)	Surface Types												
	All types	1	2	3	4	5	6	7	8	9	10	11	12
0.620–0.670	**–.76**	**–.86**	**–.77**	**–.85**	**–.62**	**–.82**	**–.91**	**–.80**	**–.67**	**–.87**	**–.31**	**–.80**	**–.79**
0.841–0.876	**–.74**	**–.88**	**–.79**	**–.87**	**–.61**	**–.87**	**–.92**	**–.82**	**–.64**	**–.87**	**–.41**	**–.80**	**–.87**
0.459–0.479	*–.16*	**–.27**	**–.49**	**–.64**	**.18**	–.06	**–.28**	–.13	**–.25**	–.24	–.09	**–.80**	**–.47**
0.545–0.565	**–.52**	**–.57**	**–.68**	**–.73**	**–.23**	**–.42**	**–.64**	**–.50**	**–.49**	**–.55**	–.13	**–.78**	**–.62**
1.230–1.250	**–.77**	**–.88**	**–.88**	**–.86**	**–.48**	**–.86**	**–.90**	**–.85**	**–.67**	**–.86**	**–.43**	**–.84**	**–.86**
1.628–1.652	**–.77**	**–.87**	**–.87**	**–.85**	**–.48**	**–.89**	**–.89**	**–.88**	**–.66**	**–.86**	**–.39**	**–.88**	**–.85**
2.105–2.155	**–.85**	**–.87**	**–.84**	**–.85**	**–.65**	**–.90**	**–.92**	**–.90**	**–.76**	**–.87**	**–.44**	**–.86**	**–.86**
0.4–0.7	**–.61**	**–.71**	**–.69**	**–.78**	**–.38**	**–.71**	**–.77**	**–.68**	**–.55**	**–.75**	**–.22**	**–.79**	**–.70**
0.7–5.0	**–.79**	**–.88**	**–.83**	**–.88**	**–.61**	**–.89**	**–.92**	**–.87**	**–.68**	**–.87**	**–.43**	**–.87**	**–.88**
0.4–5.0	**–.76**	**–.88**	**–.80**	**–.87**	**–.60**	**–.86**	**–.91**	**–.84**	**–.66**	**–.87**	**–.40**	**–.84**	**–.84**

Note: Coefficients in bold (italic) are statistically significant at $p < .01$ ($p < .05$).

Of 130 coefficients, 124 are statistically significant at the 1% level, 1 at the 5% level and only 5 are statistically insignificant at the 5% level. The blue (0.459–0.479 μm) and green (0.545–0.565 μm) bands generally have the smallest correlations while the spectral band 7 (2.105–2.155 μm) has the largest correlation. For the surface types, cambids (10) have the smallest correlations while ustepts (6) have the largest correlations. Variations of emissivity are evidently highly correlated with those of albedo.

4. Discussion

[16] Evidently, albedo and emissivity are highly correlated to each other and to the surface types. However, they have considerable variations within each given surface type, especially for the dominant soil type (orthents). Table 1 shows that all of the different surface types have means that lie within approximately one standard deviation of that of its closest neighbor.

[17] The regression in Figure 3 suggests that 58% of the total variations of emissivity can be explained by albedo and vice versa. The ANOVA analysis in Table 2 shows that 22% and 39% of the total variance of albedo and emissivity can be explained by the surface types while 78% and 61% of the variances within surface types are unexplained, respectively. Therefore, the linkage between albedo and emissivity is stronger than their association with the surface type.

[18] The within surface type variability depends on the accuracy and resolution of the soil classification map. For most surface types, the soil taxonomy map (Figure 1d) corresponds well with the soil color image (Figure 1c) in both boundaries and spatial variations, indicating its satisfactory quality. For example, shifting sands show a perfect match with those in the soil map. The dominant soil (orthents, purple in Figure 1d), which has a broad range of albedo and emissivity, shows some variations in soil color from south to north (Figure 1c), suggesting that a finer classification of soils or higher resolution mappings would improve the correlation between the soils and albedo and emissivity. Untill the reason in the weak relation between surface types and albedo/emissivity is well understood, the existing maps of surface type need to be used with caution for specification of albedo and emissivity. However, they may be adequate in larger spatial scales.

[19] The large within surface type variability may be also in part related to artifacts due to spatial misregistration of soil and satellite maps. In addition, the emissivity data are from different scenes at different dates from 2000 to 2002 while the albedo data are from the dust-free seasons in 2001. Variations of albedo and emissivity due to soil moisture may also contribute but such contribution should be very small over the study region.

[20] **Acknowledgments.** This work was funded by the NASA EOS/IDS Program (NAG5-8880).

References

Bonan, G. B., et al., The land surface climatology of the NCAR community land model coupled to the NCAR Community Climate Model, *J. Climate*, *15*, 3123–3149, 2002.

Dickinson, R. E., et al., Biosphere-Atmosphere Transfer Scheme (BATS) Version le as coupled to the NCAR Community Model, NCAR Tech. Note, NCAR/TN-387+STR, 72 pp., *Natl. Cent. Atmos. Res*., Boulder, CO, 1993.

FAO, 1994: *Digitized Soil Map of the World (version 2.0) derived from the FAO/UNESCO Soil Map of the World*, Food and Agriculture Organization, Rome, Italy, 1994.

Friedl, M. A., et al., Global land cover from MODIS: Algorithms and early results, *Remote Sens. Environ.*, *83*, 287–302, 2002.

Ogawa, K., et al., Estimation of land surface window (8–12 μm) emissivity from multispectral thermal infrared remote sensing - A case study in a part of Sahara Desert, *Geophys. Res. Lett.*, *30*, 1067, doi:10.1029/2002GL016354, 2003a.

Ogawa, K., et al., Mapping of land surface window (8–12 μm) emissivity from ASTER thermal data, *Proceedings for International Geoscience and Remote Sensing Symposium*, INT-C04 03.0890, Toulouse, France, July, 2003b.

Schaaf, C. B., et al., First operational BRDF, albedo, and nadir reflectance products from MODIS, *Remote Sens. Environ.*, *83*, 135–148, 2002.

Soil Survey Staff, *Soil Taxonomy: A basic system of soil classification for making and interpreting soil surveys, 2nd Edition, Agriculture Handbook, No. 436*, pp. 871, USDA/Natural Resources Conservation Service, 1999.

Tian, Y., et al., Radiative transfer based scaling of LAI/FPAR retrievals from reflectance data of different resolutions, *Remote Sens. Environ.*, *84*, 143–159, 2002.

Tsvetsinskaya, E. A., et al., Relating MODIS-derived surface albedo to soils and rock types over Northern Africa and the Arabian peninsula, *Geophys. Res. Lett.*, doi:10.1029/2001GL014096, 2002.

Zeng, X., et al., Coupling of the Common Land Model to the NCAR Community Climate Model, *J. Clim.*, *14*, 1832–1854, 2002.

Zhou, L., et al., Comparison of seasonal and spatial variations of albedos from MODIS and Common Land Model, *J. Geophys. Res.*, *108*(D15), 4488, doi:10.1029/2002JD003326, 2003.

L. Zhou, R. E. Dickinson, and Y. Tian, School of Earth and Atmospheric Sciences, Georgia Institute of Technology, Atlanta, GA 30332, USA. (lmzhou@eas.gatech.edu)

K. Ogawa and T. Schmugge, USDA/ARS Hydrology and Remote Sensing Lab., Beltsville, MD 20705, USA.

M. Jin, Department of Meteorology, University of Maryland, College Park, MD 20742, USA.

E. Tsvetsinskaya, Department of Geography, Boston University, Boston, MA 02215, USA.